Kagomé Ice State in the Dipolar Spin Ice $Dy_2Ti_2O_7$

Y. Tabata,[1] H. Kadowaki,[2] K. Matsuhira,[3] Z. Hiroi,[4] N. Aso,[5] E. Ressouche,[6] and B. Fåk[6]

[1]*Graduate School of Science, Osaka University, Toyonaka, Osaka 560-0043, Japan*
[2]*Department of Physics, Tokyo Metropolitan University, Hachioji-shi, Tokyo 192-0397, Japan*
[3]*Department of Electronics, Kyushu Institute of Technology, Kitakyushu 804-8550, Japan*
[4]*Institute for Solid State Physics, University of Tokyo, Kashiwa, Chiba 277-8581, Japan*
[5]*NSL, Institute for Solid State Physics, University of Tokyo, Tokai, Ibaraki 319-1106, Japan*
[6]*CEA, Département de Recherche Fondamentale sur la Matiére Condensée, SPSMS, 38054 Grenoble, France*

(Received 13 July 2006; published 21 December 2006)

We have investigated the kagomé ice behavior of the dipolar spin-ice compound $Dy_2Ti_2O_7$ in a magnetic field along a [111] direction using neutron scattering and Monte Carlo simulations. The spin correlations show that the kagomé ice behavior predicted for the nearest-neighbor interacting model, where the field induces dimensional reduction and spins are frustrated in each two-dimensional kagomé lattice, occurs in the dipole interacting system. The spins freeze at low temperatures within the macroscopically degenerate ground states of the nearest-neighbor model.

DOI: 10.1103/PhysRevLett.97.257205 PACS numbers: 75.10.Hk, 05.50.+q, 75.25.+z

Geometrically frustrated spin systems have been investigated for decades because of their fascinating magnetic properties [1–5]. An Ising model on a cubic pyrochlore lattice consisting of spins parallel to local $\langle 111 \rangle$ easy axes was shown to exhibit macroscopic degeneracy in the ground states [1,6,7] in the same way as the proton disorder in water ice does [8]. The local easy axis, *ferromagnetic* nearest-neighbor (NN) exchange interaction, and the geometry of corner sharing tetrahedra give rise to frustration in this system. Since the local ''two-in and two-out'' spin configuration of the ground states simulates the ''ice rule'' in water ice, the Ising model is referred to as ''spin ice'' [1].

Frustrated behavior attributable to the NN ferromagnetic spin-ice model was discovered in pyrochlore oxides, e.g., $R_2Ti_2O_7$, $R_2Sn_2O_7$ (R = Dy, Ho) [6,7,9,10], where the observed residual entropy agrees with the Pauling estimate for water ice [7]. However, spins in these oxides interact dominantly by the dipolar interaction. Hence, they are represented by another Ising model with a dominant dipolar interaction, referred to as dipolar spin ice [11]. It was a puzzle why the dipolar spin ice shows the spin-ice behavior predicted for the NN model. This was solved by Monte Carlo (MC) simulation studies [11–13], showing that the dipolar interaction brings about an effective NN ferromagnetic coupling. In addition, it was shown that the long-range dipolar interaction only slightly lifts the degeneracy of the ground-state manifold of the NN spin-ice model, and spins freeze within this manifold at low temperatures and never reach the true ground state [12,13]. The simulations also reproduce experimental observations of the dipolar spin-ice compounds [11,13,14]. More recently, an elegant analytical understanding has been exploited using an argument of projective equivalence [15].

By applying magnetic fields to the NN spin-ice model, the macroscopic degeneracy of the ground states can be partly or fully lifted, depending on the field direction and magnitude [7,16]. For a field parallel to a [111] direction, along which the pyrochlore lattice is alternating stacking of kagomé and triangular layers [see Fig. 1(a)], the field with intermediate strengths partly lifts the degeneracy and simultaneously induces decoupling of spins between the layers. In these ground states, spins on the triangular layers are parallel to the field, and spins on the kagomé layers retain macroscopic degeneracy preserving the two-in and two-out configuration at each tetrahedron [see Fig. 1(b)] [17]. The ground states on each kagomé layer can be mapped onto those of an exactly solvable dimer model in two dimensions [18–20]. At low temperatures, by neglecting excited states with an energy gap, one can expect icelike behavior of the spins on the kagomé lattice, referred to as ''kagomé ice'' [17].

For the dipolar spin ice $Dy_2Ti_2O_7$, experiments with a field along [111] were performed [17,21–23]. It was shown that the magnetization plateau is consistent with the predictions of the kagomé ice behavior for the NN model [17,23]. However, the residual entropy plateau, another important point for proving the kagomé ice, has not been definitely shown by the specific heat measurements [17,21,22] because of experimental difficulties [21]. In addition, effects of the long-range nature of the dipolar interaction have not been clarified for the kagomé ice state. In this work, we performed neutron scattering experiments on $Dy_2Ti_2O_7$ with a field along [111] in the conjectured kagomé ice regime, aiming at microscopic demonstration of the kagomé ice state. We compared the neutron data with MC simulations based on the dipolar spin-ice model [11,13]. The simulations reproduce the main characteristics of the kagomé ice: the residual entropy, the spin correlations close to the wave vector $(\frac{2}{3}, -\frac{2}{3}, 0)$, and the field-induced dimensional reduction, consistent with observations.

Most of the neutron scattering experiments were performed on the triple-axis spectrometer GPTAS at Japan

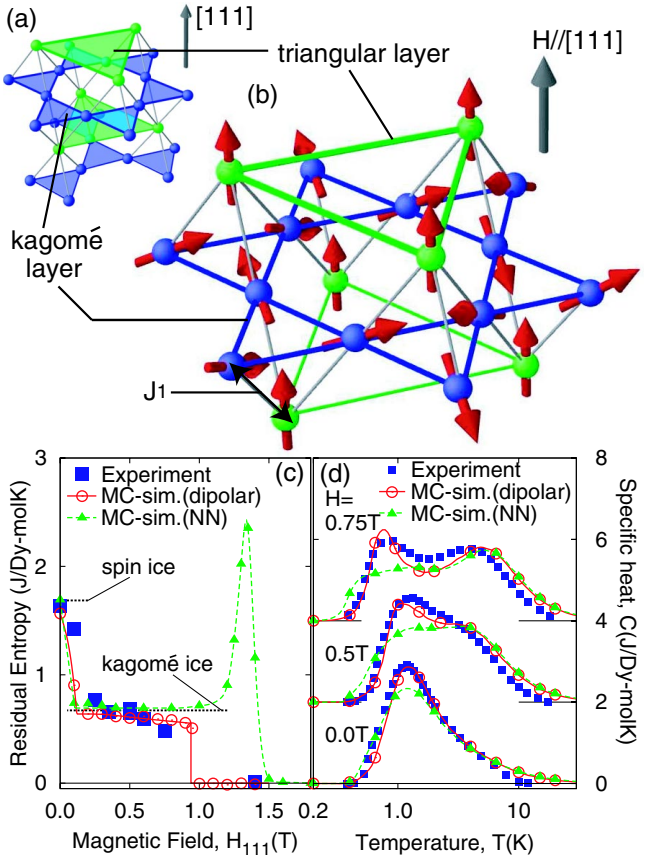

FIG. 1 (color online). (a) The pyrochlore lattice is alternating stacking of kagomé and triangular layers along a [111] direction. (b) A spin configuration of the kagomé ice state is shown. (c) The observed [21] and calculated residual entropies are plotted as a function of magnetic field. The calculated entropy for the NN model [20] is $S(T = 0.1\ \mathrm{K})$, which is temperature-dependent in the peaked region. Dotted lines represent the precise values of the spin-ice and kagomé ice states for the NN model [18,19]. (d) Temperature dependence of observed [21] and calculated specific heat at $H = 0$, 0.5, and 0.75 T.

Atomic Energy Agency. A single crystal sample of $Dy_2Ti_2O_7$ used in this work was $22 \times 3.1 \times 0.58\ \mathrm{mm}^3$ in size. Its long direction is parallel to a [111] direction, which ensures a negligibly small demagnetization effect. The sample was mounted in a dilution refrigerator so as to measure the scattering plane perpendicular to the [111] direction. A scan along the [111] direction was carried out on the lifting-arm two-axis diffractometer D23 CEA-CRG at Institute Laue-Langevin. All the data shown are corrected for background and absorption. The MC simulations were carried out using a supercomputer at Institute for Solid State Physics, University of Tokyo. A standard Metropolis algorithm with single-spin-flip dynamics was used in our simulations. The long-range dipolar interaction was handled by a method [24] equivalent to the Ewald method [11,13]. We carried out the simulations up to 38 400 spins with up to 6×10^5 MC steps per spin.

We adopted the Hamiltonian used in Refs. [11,25]:

$$\mathcal{H} = -\mu_{\mathrm{eff}} \sum_{i,a} \boldsymbol{S}_i^a \cdot \boldsymbol{H} - \sum_{\langle (i,a),(j,b) \rangle} J_{i,a;j,b} \boldsymbol{S}_i^a \cdot \boldsymbol{S}_j^b + D r_{\mathrm{nn}}^3 \sum \left[\frac{\boldsymbol{S}_i^a \cdot \boldsymbol{S}_j^b}{|\boldsymbol{R}_{ij}^{ab}|^3} - \frac{3(\boldsymbol{S}_i^a \cdot \boldsymbol{R}_{ij}^{ab})(\boldsymbol{S}_j^b \cdot \boldsymbol{R}_{ij}^{ab})}{|\boldsymbol{R}_{ij}^{ab}|^5} \right], \quad (1)$$

where $\boldsymbol{S}_i^a$ represents the spin vector parallel to the local $\langle 111 \rangle$ easy axis, with $|\boldsymbol{S}_i^a| = 1$ at the sublattice site a in the unit cell of the fcc lattice site i. The first term is the Zeeman interaction between the spins possessing the effective moment $\mu_{\mathrm{eff}} \simeq 10\ \mu_B$ and the magnetic field $\boldsymbol{H}$. The second and third terms are the exchange and dipolar interactions, respectively. For the NN ferromagnetic spin-ice model, there is only one exchange coupling constant $J_1 > 0$ and $D = 0$.

It is well established that the low temperature behavior of $Dy_2Ti_2O_7$ can be approximately reproduced by a single-spin-flip MC simulation based on the dipolar spin-ice model [11–13,25] except a few observations. For this model, the dipolar interaction with $D = 1.41$ K and the Zeeman interaction are the dominant terms. The weaker exchange interactions consist of the NN antiferromagnetic interaction with $J_1 = -3.72$ K and smaller second- and third-neighbor couplings with $J_2 = 0.1$ and $J_3 = -0.03$ K, respectively. The very weak J_3 becomes important for determining the ground state within the degenerate states when the field is along [112], because larger interactions balance each other [25,26]. Another balancing occurs for the [111] field close to the spin-flop transition [see Fig. 2(I)], which allowed us to determine J_2 by a fit of the T dependence of the specific heat $C(H = 0.75\ \mathrm{T})$ [see Fig. 1(d)] to the simulation [24].

The kagomé ice behavior in $Dy_2Ti_2O_7$ was suggested by the residual entropy measurement [17,21] for fields close to $H = 0.5$ T as shown in Fig. 1(c). We calculated the residual entropy using MC simulation of the dipolar spin-ice model, where $C(H)/T$ is integrated over $0.2 \leq T \leq 200$ K. The MC calculations are shown in Figs. 1(c) and 1(d) together with those using the NN spin-ice model with ferromagnetic $J_1 = 4.5$ K [20]. The computation agrees with the experiment around $H \sim 0.5$ T and shows more clearly the plateau behavior than the experiment [21]. The low temperature entropy $S(T = 0.1\ \mathrm{K})$ of the NN spin-ice model [20], showing a peaked structure at a higher field ($H \sim 1.35$ T), indicates that the discontinuous decrease of the residual entropy at $H \sim 0.9$ T, accompanying the spin-flop transition [23], is brought about by the long-range dipolar interaction.

The plateau of the residual entropy around $H \sim 0.5$ T of the dipolar spin-ice model is slightly smaller than that of the NN model. This suggests that the kagomé ice ground-state manifold of the NN model is weakly lifted by the dipolar interaction. For the origin of the kagomé ice behavior of $Dy_2Ti_2O_7$, one naturally expects that spins freeze within these nearly degenerate ground states owing to the

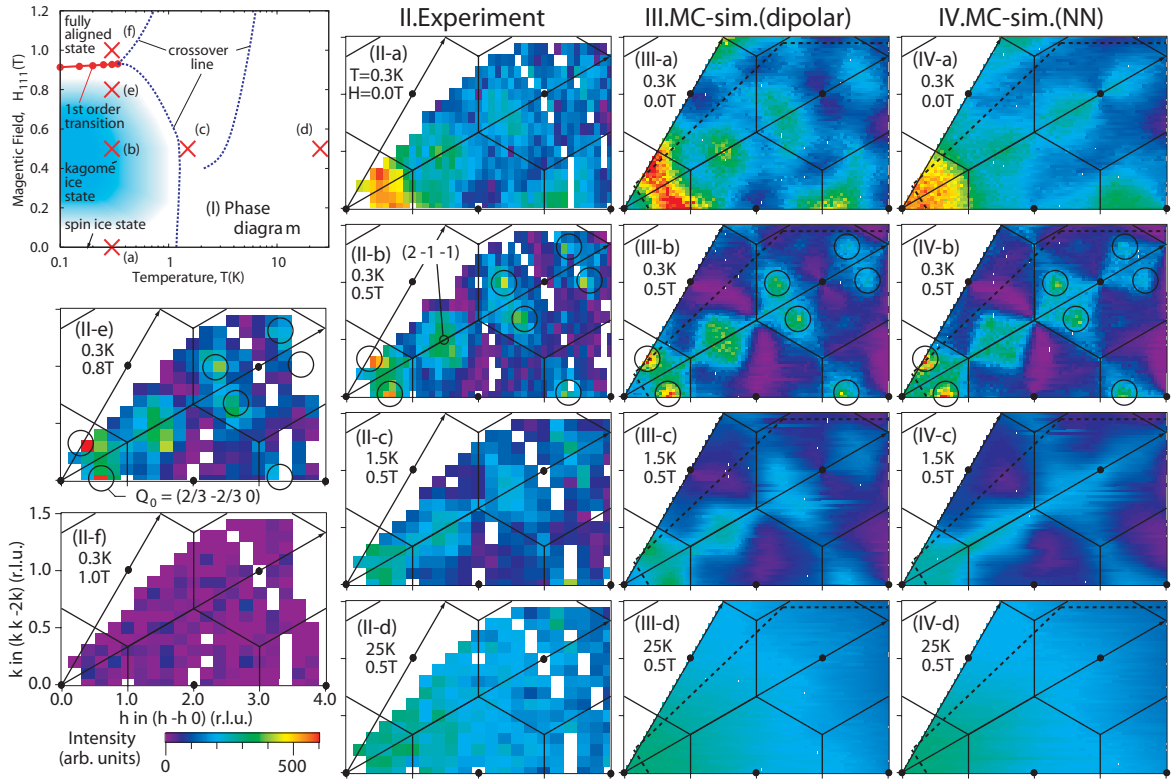

FIG. 2 (color). (I) HT phase diagram of $Dy_2Ti_2O_7$ obtained from the magnetization and the specific heat measurements [21,23]. The kagomé ice state is observed in the blue region. The red solid line represents the first-order spin-flop transition. (II)–(IV) Neutron intensity patterns in the scattering plane perpendicular to the [111] direction are shown for several temperatures and fields denoted by crosses in (I). In (II), experimental results for $Dy_2Ti_2O_7$ are shown. Calculations using the MC simulation based on the dipolar and NN spin-ice models are shown in (III) and (IV), respectively.

high energy barriers for breaking the two-in and two-out ice rule [12]. This mechanism can be microscopically investigated by observing spin correlations using neutron scattering techniques.

In Fig. 2(II), we show neutron intensity patterns in the scattering plane perpendicular to the [111] direction at several points in the HT plane denoted by crosses in Fig. 2(I). The low temperature data at $T = 0.3$ K show definite differences between the spin-ice state at $H = 0$ [Fig. 2(II)(a)], the kagomé ice state at $H = 0.5$ and 0.8 T [Figs. 2(II)(b) and 2(II)(e)], and the fully aligned state at $H = 1$ T [Fig. 2(II)(f)], where very weak scattering intensity implies that very small spin fluctuations are left above the spin-flop transition. We note that the intensity peak observed for the kagomé ice state [Figs. 2(II)(b) and 2(II)(e)] at the wave vector $\boldsymbol{Q}_0 = (\frac{2}{3}, -\frac{2}{3}, 0)$, denoted by black circles, is a characteristic of the kagomé ice state. This spin correlation was found in the exact ground states of the NN spin-ice model [18].

In Figs. 2(III) and 2(IV), we show scattering intensities calculated by MC simulations based on the dipolar and NN spin-ice models, respectively. The simulations for the spin-ice state [Figs. 2(III)(a) and 2(IV)(a)], which are consistent with previous results [14,27], confirm that the agreement with experiments [Fig. 2(II)(a)] is improved by taking account of the dipolar interaction. In contrast to this, the simulations for the kagomé ice state [Figs. 2(III)(b) and 2(IV)(b)] show almost the same pattern to the naked eye and agree well with the experiment [Fig. 2(II)(b)]. As noticed previously, the field induces decoupling of the spins between the kagomé layers for the NN model. This field-induced dimensional reduction is confirmed by no Q dependence of the calculated intensity pattern [Fig. 2(IV)(b)] along the [111] direction. For the dipolar model, we also observed little Q dependence of the calculated intensity pattern [Fig. 2(III)(b)] along the [111] direction and, hence, conclude that the spin correlations show quasi-two-dimensional character in the kagomé ice state. As temperature is increased at the typical field $H =$ 0.5 T of the kagomé ice state, the experimental intensity patterns [Figs. 2(II)(c) and 2(II)(d)] are consistent with the simulations [Figs. 2(III)(c), 2(III)(d), 2(IV)(c), and 2(IV)(d)]. From these results, we conclude that the degeneracy of the kagomé ice ground states of the NN spin-ice model is almost identically preserved for the dipolar spin-ice model and for $Dy_2Ti_2O_7$, providing microscopic evidence for the kagomé ice behavior of this compound.

In order to study the spin correlations around $\boldsymbol{Q}_0$ at $H =$ 0.5 T, we performed scans along the $(h, -h, 0)$ line and plot the results in Fig. 3, where the MC calculations of the

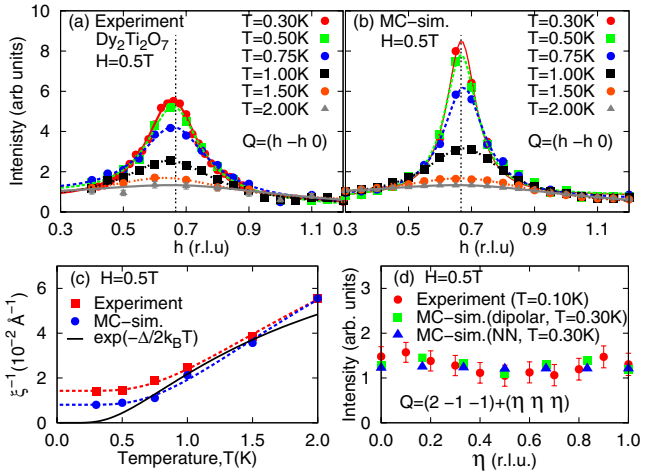

FIG. 3 (color online). Q scans along the $(h, -h, 0)$ line through $\boldsymbol{Q}_0$ at $H = 0.5$ T: (a) experimental and (b) MC simulation results based on the dipolar model. Curves are fits to Lorentzian functions. (c) Temperature dependence of the inverse correlation length ξ^{-1} obtained by the fits. The dotted lines are guides to eyes. The solid line represents the exponential T dependence $\exp(-\Delta/2k_BT)$ described in the text. (d) Q scan along the [111] direction from $(2\bar{1}\,\bar{1})$ [Fig. 2(II)(b)].

dipolar model are also shown. One can see from Fig. 3(a) that the spin correlations of $Dy_2Ti_2O_7$ cease to develop around $T = 0.5$ K. This disagrees with the theory of the NN model [18], where it was argued that the correlation length diverges exponentially as $\exp(\Delta/2k_BT)$ $(T \to 0)$, where Δ is a gap energy, in the thermal equilibrium state. The nondivergence of the spin correlations for $Dy_2Ti_2O_7$ can be ascribed to spin freezing due to the barrier for breaking the ice rule. As discussed in Ref. [12] for the spin-ice state, the single-spin-flip dynamics of the MC simulation becomes nonergodic at low temperatures, and, hence, the simulated system does not reach a thermal equilibrium state within practical MC steps, as well as $Dy_2Ti_2O_7$ does not within experimental time scales. In fact, the simulated system also shows freezing around $T = 0.7$ K, which does not necessarily agree with the experiment because of the difference of the spin-flip dynamics between the simulated system and $Dy_2Ti_2O_7$. To observe the two-dimensional spin correlations in the kagomé ice state, we performed a Q scan along the [111] direction from $(2\bar{1}\,\bar{1})$ [see Fig. 2(II)(b)]. The result together with the MC simulations of the two models are shown in Fig. 3(d). These experimental data, being consistent with the simulations within the experimental error, suggest the two-dimensional nature of the kagomé ice state in $Dy_2Ti_2O_7$.

Finally, we note that a surprising fact revealed by the present numerical study is the high similarity of the spin correlations, shown in Figs. 2(III) and 2(IV), between the NN and dipolar models especially for the kagomé ice state. In view of the theoretical work [11,15] explaining the equivalence of the NN and dipolar models for the spin-ice state, there may be a similar enlightening argument also for the kagomé ice state.

In summary, we have investigated the kagomé ice behavior and field-induced dimensional reduction of the dipolar spin ice $Dy_2Ti_2O_7$ in a magnetic field along the [111] direction using neutron scattering. The observed spin correlations were analyzed by MC simulations based on the dipolar and NN spin-ice models. For fields around $H \sim 0.5$ T, spins freeze within the degenerate kagomé ice ground states of the NN model, which are weakly lifted by the dipolar interaction, and consequently exhibit kagomé ice behavior.

[1] S. T. Bramwell and M. J. P. Gingras, Science **294**, 1495 (2001).
[2] J. S. Gardner *et al.*, Phys. Rev. Lett. **82**, 1012 (1999).
[3] J. S. Gardner *et al.*, Phys. Rev. Lett. **83**, 211 (1999).
[4] I. Mirebeau *et al.*, Nature (London) **420**, 54 (2002).
[5] S.-H. Lee *et al.*, Nature (London) **418**, 856 (2002).
[6] M. J. Harris *et al.*, Phys. Rev. Lett. **79**, 2554 (1997).
[7] A. P. Ramirez *et al.*, Nature (London) **399**, 333 (1999).
[8] L. Pauling, J. Am. Chem. Soc. **57**, 2680 (1935).
[9] H. Kadowaki, Y. Ishii, K. Matsuhira, and Y. Hinatsu, Phys. Rev. B **65**, 144421 (2002).
[10] K. Matsuhira, Y. Hinatsu, K. Tenya, and T. Sakakibara, J. Phys. Condens. Matter **12**, L649 (2000).
[11] B. C. den Hertog and M. J. P. Gingras, Phys. Rev. Lett. **84**, 3430 (2000).
[12] R. G. Melko, B. C. den Hertog, and M. J. P. Gingras, Phys. Rev. Lett. **87**, 067203 (2001).
[13] R. G. Melko and M. J. P. Gingras, J. Phys. Condens. Matter **16**, R1277 (2004).
[14] S. T. Bramwell *et al.*, Phys. Rev. Lett. **87**, 047205 (2001).
[15] S. V. Isakov, R. Moessner, and S. L. Sondhi, Phys. Rev. Lett. **95**, 217201 (2005).
[16] M. J. Harris *et al.*, Phys. Rev. Lett. **81**, 4496 (1998).
[17] K. Matsuhira, Z. Hiroi, T. Tayama, S. Takagi, and T. Sakakibara, J. Phys. Condens. Matter **14**, L559 (2002).
[18] R. Moessner and S. L. Sondhi, Phys. Rev. B **68**, 064411 (2003).
[19] M. Udagawa, M. Ogata, and Z. Hiroi, J. Phys. Soc. Jpn. **71**, 2365 (2002).
[20] S. V. Isakov, K. S. Raman, R. Moessner, and S. L. Sondhi, Phys. Rev. B **70**, 104418 (2004).
[21] Z. Hiroi, K. Matsuhira, S. Takagi, T. Tayama, and T. Sakakibara, J. Phys. Soc. Jpn. **72**, 411 (2003); as pointed out in this reference, experimental determination of residual entropy was difficult because of subtractions of the phonon contribution and the unknown background.
[22] R. Higashinaka, H. Fukazawa, K. Deguchi, and Y. Maeno, J. Phys. Soc. Jpn. **73**, 2845 (2004).
[23] T. Sakakibara, T. Tayama, Z. Hiroi, K. Matsuhira, and S. Takagi, Phys. Rev. Lett. **90**, 207205 (2003).
[24] Details of the method of the present MC simulation are described in H. Kadowaki *et al.* (to be published).
[25] J. P. C. Ruff, R. G. Melko, and M. J. P. Gingras, Phys. Rev. Lett. **95**, 097202 (2005).
[26] R. Higashinaka and Y. Maeno, Phys. Rev. Lett. **95**, 237208 (2005).
[27] T. Fennell *et al.*, Phys. Rev. B **70**, 134408 (2004).